Adsorption 9: 67–76, 2003

Thermal-Adsorptive Concentration

GOPALAN NATARAJAN* AND PHILLIP C. WANKAT**
School of Chemical Engineering, Purdue University, West Lafayette, IN 47907-1283, USA
wankat@ecn.purdue.edu

Received January 18, 2002; Revised June 3, 2002; Accepted June 27, 2002

Abstract. Methods for concentrating dilute fluids using adsorption followed by partial thermal regeneration were studied using the simulation package ADSIM. The systems studied were NaCl in liquid water on Amberlite XD-2 resin and benzene vapor in nitrogen on activated carbon. Cycles studied included counter-current regeneration with pure hot fluid, co-current regeneration with pure hot fluid, a new process called Hot Feed Addition (HFA) consisting of co-current regeneration with pure hot fluid followed by hot feed, and cycling zone adsorption (co-current alternating hot and cold feeds with no pure regeneration fluid). The optimum system depends upon the conditions of the system and the value function chosen to evaluate the systems. For example, for benzene in nitrogen with hot regeneration gas at 467.4 K, cycling zone adsorption used no carrier gas, had the most concentrated benzene stream and a very pure nitrogen product, but the energy use was greater than the other processes. For liquid systems counter-current operation could produce the purest product, but regenerant requirements were high. With slightly lower purity requirements HFA reduced solvent usage and increased the concentration of the concentrated waste stream. For the liquid system all processes used approximately 3% or less of the energy that would be required for evaporation.

Keywords: adsorption, cycling zone adsorption, thermal-swing adsorption

Introduction

In industrial chemical processes, it is not unusual to have process/waste streams that contain extremely low concentrations of a valuable or toxic component that needs to be removed. With environmental regulations becoming stricter, new methods of reducing the concentration of pollutants in plant waste streams are needed. Conversely, if solvent usage is a concern, then pure solvent recovery and recycle can reduce long-term process operating costs for both inexpensive solvents (like water), and more exotic ones. A reduction in the volume of processed fluid alone can result in significant savings in capital and operating costs. An unfortunate, but unavoidable, reality of such situations is that large volumes of solution have to be processed in order to recover appreciable amounts of the component of interest. Thus, concentrating the solution would be very advantageous from a storage and disposal point of view. However, many methods for concentrating dilute solutions are either very energy intensive (evaporation) or often do little to reduce volume (extraction).

Adsorption is admirably suited for concentrating dilute solutions since it allows a particular component to be selectively separated with a minimum of energy input. The system can be tailored to a variety of solutes by picking an adsorbent with a high affinity for the solute of interest. Adsorbent beds are often regenerated by using large temperature swings to change the amount of solute adsorbed. Adsorption equilibria behave such that the solute adsorbs more strongly at a low temperature and less strongly at a high temperature. Accordingly, material that is adsorbed to a bed of particles will tend to desorb from the bed when subjected to a high temperature.

*Present address: ExxonMobil Corp., Baytown, TX, USA.
**To whom correspondence should be addressed.

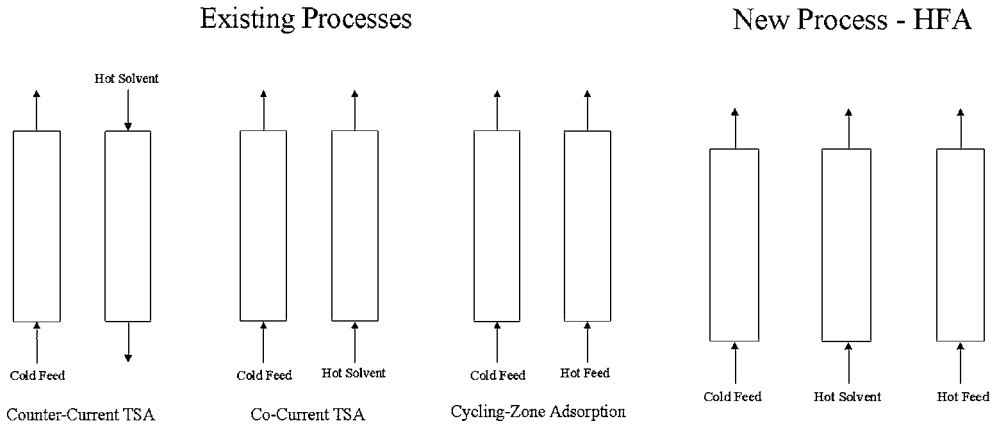

Figure 1. Existing and new adsorption processes.

The major thermal-cycling techniques used today are shown in Fig. 1. Counter-current Thermal-Swing Adsorption (TSA) is the most common commercially. In counter-current TSA, the solute is first adsorbed at a low temperature and is desorbed by a counter flow of hot solvent or purge gas. A cooling step can also be employed, but was not included in this study. TSA can also be operated as a co-current system, although this is unusual (Wankat, 1990). TSA has an advantage over more traditional concentration/purification methods since the energy requirements are comparatively low. The only energy input necessary is to heat the solvent or purge gas to the desired desorption temperature. The major limitation of TSA is that it is only economically feasible for dilute feeds due to the relatively large amounts of solvent/purge gas required to effectively process concentrated feed streams (Wankat, 1990). Co-current TSA configurations using recycle for the regeneration step have been studied and show promising results (Kayser and Knaebel, 1987; Matz and Knaebel, 1991).

Cycling Zone Adsorption (CZA) is a co-current process that operates by alternating between hot and cold feed solutions to concentrate the solute (Knaebel and Pigford, 1983). Under favorable conditions, a phenomenon called focusing, or the guillotine effect, occurs which results in large increases in concentration of the concentrated product and a very pure solvent or carrier gas product (Tondeur et al., 1981; Wankat, 1990). The inherent disadvantage of CZA is that when focusing does not occur it is impossible to obtain very pure solvent or carrier gas as a product. Since the desorption step uses the feed solution there can be a significant amount of solute in the solvent or carrier gas product.

These limitations lead to the new method proposed in this work. Dubbed "Hot Feed Addition" (HFA), it combines the principles of co-current TSA and CZA. HFA is a co-current process that cycles between cold feed, hot solvent and hot feed. This allows for distinct periods of concentrated solution and pure solvent. Much of the reduction in solvent or purge gas use seen in CZA is retained while gaining the potential benefit of purer solvent recovery. This novel design is actually the more general process, with co-current TSA and CZA being extreme cases of HFA. The configurations of the four systems studied are depicted in Fig. 1. Both liquid and gas applications were studied. For the liquid system, the purification of brackish water (sodium chloride solution) was investigated. For the gas system, the concentration of trace benzene in nitrogen was used to represent benzene removal from air.

Theory and Model Design

The mass and energy balances for non-isothermal fixed bed adsorption can be derived by writing differential balances around the solid and fluid phases. For the mass balance, the major assumptions that need to be made are that radial gradients are negligible, no chemical reactions (other than chemisorption) are taking place and mass transfer follows a linear driving force model. After making these assumptions, the mass balance is

$$\frac{\partial(vc)}{\partial z} - \varepsilon E_z \frac{\partial^2 c}{\partial z^2} + \varepsilon \frac{\partial c}{\partial t} + \rho_p (1-\varepsilon)\frac{\partial \bar{q}}{\partial t} = 0 \quad (1)$$

with the mass transfer relation given as

$$\rho_p(1-\varepsilon)\frac{\partial q}{\partial t} = k_m a_p(c - c^*) \tag{2}$$

The overall energy balance can be written as

$$\varepsilon\rho_f C_{p,f}\frac{\partial(vT)}{\partial z} - \varepsilon E_{zT}\rho_f C_{pf}\frac{\partial^2 T}{\partial z^2} + \varepsilon\rho_f C_{p,f}\frac{\partial T}{\partial t} + (1-\varepsilon)\rho_\rho C_{p,s}\frac{\partial \bar{T}_s}{\partial t} = \rho_p(\Delta H)\frac{\partial q}{\partial t} \tag{3}$$

The equilibrium data used in this research were correlated with the Langmuir Isotherm

$$q = \frac{A(T)\,c}{1 + B(T)\,c} \tag{4}$$

Both isotherm parameters follow a pseudo-Arrhenius temperature dependence.

$$A(T) = A_1 \cdot e^{\frac{A_2}{T}} \tag{5}$$

$$B(T) = B_1 \cdot e^{\frac{B_2}{T}} \tag{6}$$

Thus, as the temperature increases, the amount adsorbed decreases. Pressure drop was determined from the Carmen-Kozeny equation. The mass transfer coefficient for the liquid system was 0.30639 1/s (Knaebel and Pigford, 1983) while the mass transfer coefficient for the gas system was calculated using correlations (Schork and Fair, 1988). The regeneration temperature for the gas system was determined as the characteristic temperature (Basmadjian et al., 1975) at which focusing occurs,

$$\left.\frac{\partial q}{\partial y}\right|_{y=0} = \frac{C_{p,s}}{C_{p,f}} \tag{7}$$

Obviously, equations of this complexity have to be solved by numerical techniques unless a large number of simplifying assumptions are valid. The adsorption simulator ADSIM^{TM}, by Aspen Technology, Inc. was used. The simulations were performed on a Pentium II 450 MHz computer with 256 MB of RAM. ADSIM directly solves the complete mass and energy balances numerically with the appropriate boundary conditions using a method of lines technique. The spatial derivatives are discretized with algebraic approximations, resulting in a set of ordinary differential and algebraic equations. The discretization is done over a user-defined number of grid points (nodes). Since the algebraic approximation of the first order spatial derivatives is the most difficult part of the calculation, ADSIM provides several finite differencing algorithms for use, depending on the degree of non-linearity of the system and the steepness of the discontinuities (shocks). The simulation flowsheet consists of one adsorption bed, two feed units (one for the cold dilute feed solution, the other for the hot solvent or hot feed in CZA), two product units (one to collect the concentrated product and the other to collect the solvent product) and four valves to control the flow. The data and cycle steps for these systems were obtained from the literature (Knaebel and Pigford, 1983; Schork and Fair, 1988; Yun et al., 2000), and are given in detail elsewhere (Natarajan, 2001).

Simulation Results: Liquid System

The liquid system simulations all used a feed with a composition of $c_F = 0.174$ wt% sodium chloride in water at $T_F = T_c = 25°C$. The solvent used was pure water at a temperature of $T_h = 90°C$. The resin was Amberlite XD-2, which is an amphoteric resin that is temperature sensitive (Knaebel and Pigford, 1983). The base hot addition period for all configurations was 6000 sec. per cycle. All configurations reached cyclic steady state within two cycles. The outlet composition and temperature profiles of the co-current salt TSA simulation are given in Fig. 2. As expected, the concentration suddenly jumps as the thermal wave passes through the column. The maximum composition is 1.557 wt%, the average composition of the peak is 0.611 wt% and the average salt concentration of the solvent product is 0.00445 wt%.

The outlet composition profile and the temperature at the top of the column for counter-current TSA are shown in Fig. 3. Note that the outlet concentration is at the top of the column for the pure product and at the bottom for the concentrated product. The maximum concentration is 1.562 wt%, the average peak composition is 0.667 wt% and the solvent product composition is 5.403E-4 wt%. As with co-current TSA, the temperature and concentration changes in the column are quite rapid. In fact, the profiles are similar to the co-current profiles, save for the "shoulder" at the feed concentration at about 24,000 sec. that is caused by the time it takes the thermal wave to traverse the column.

The outlet composition of the salt CZA simulation is given in Fig. 4. The maximum composition of the peak at cyclic steady state is 1.557 wt%. The average composition of the peak is 0.591 wt%, which is less than

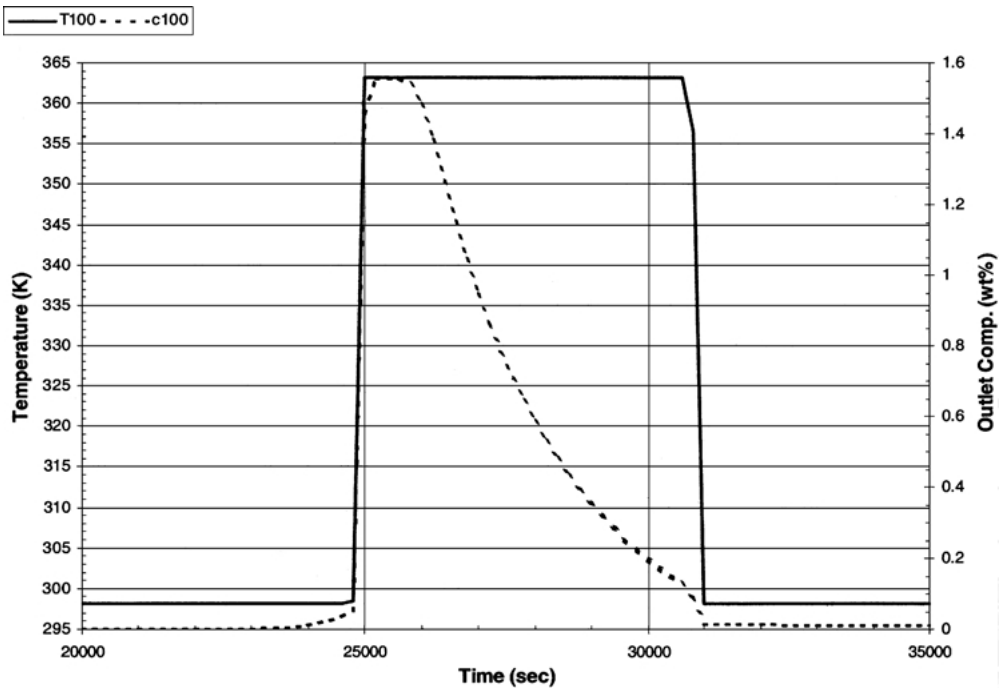

Figure 2. Co-current TSA composition and temperature profiles for dilute aqueous sodium chloride feed. Cold feed (25°C) for 24,225 sec. and pure hot water (90°C) for 6000 sec.

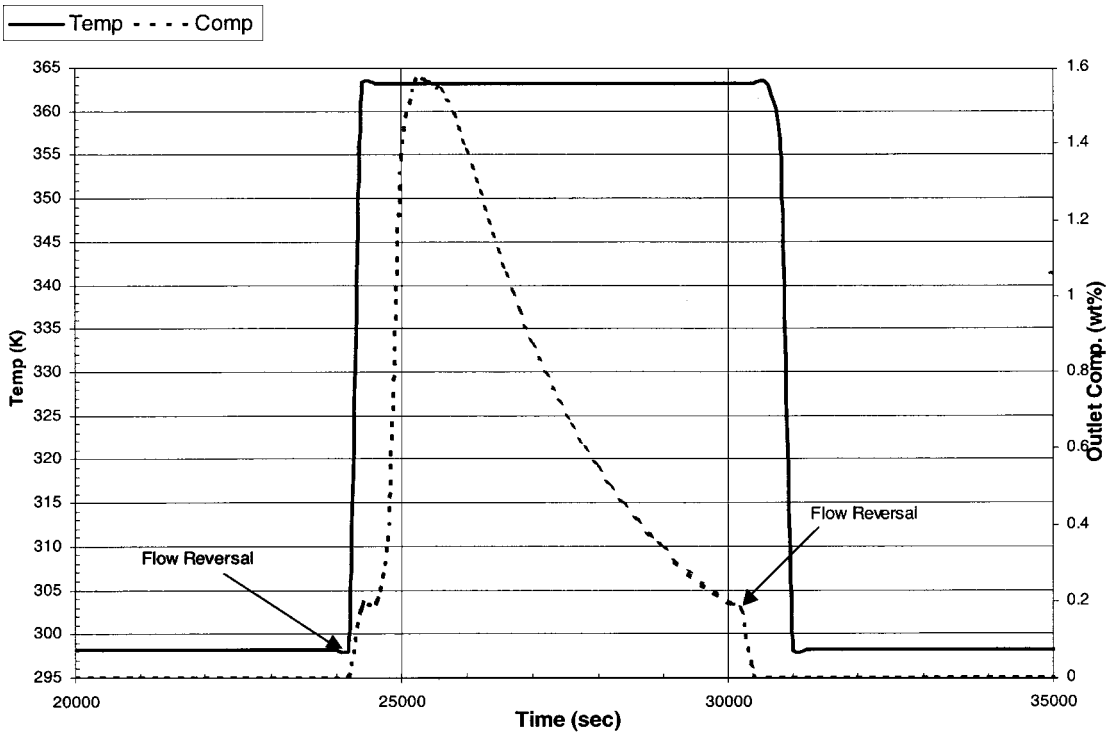

Figure 3. Counter-current TSA outlet composition profile and temperature at the top of the column for dilute aqueous sodium chloride feed. Cold feed (25°C) for 24,945 sec. and pure hot water (90°C) for 6000 sec.

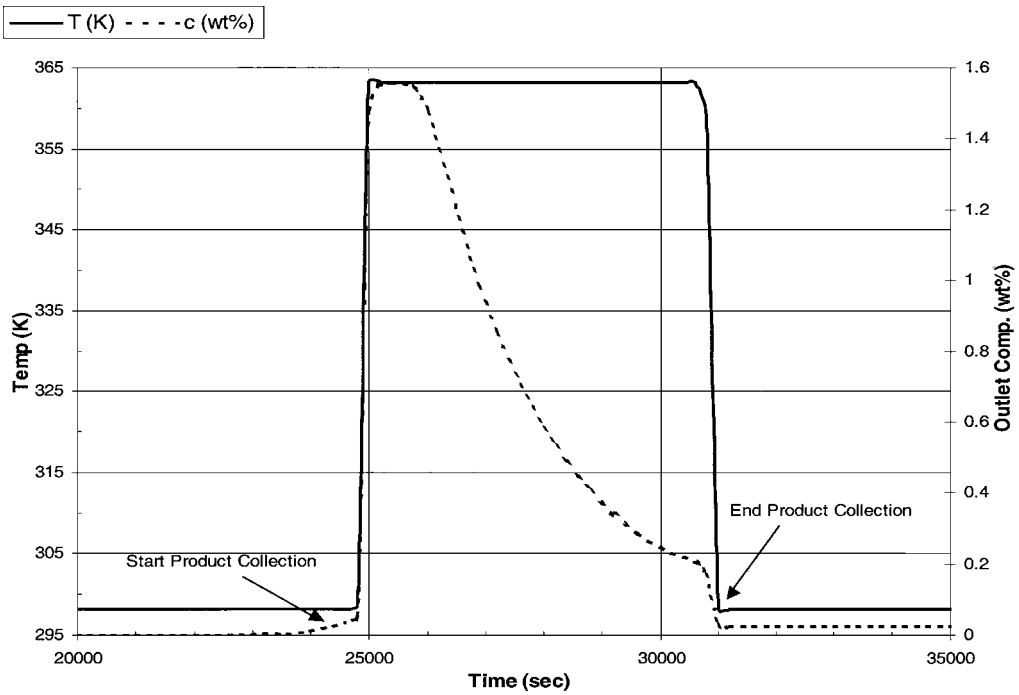

Figure 4. CZA composition and temperature profiles for dilute aqueous sodium chloride feed. Cold feed (25°C) for 19,610 sec. and pure hot feed (90°C) for 6000 sec.

for co-current TSA. However, the major differentiating factor between TSA and CZA is not the composition of the concentrated product, but rather the purity of the solvent product. The CZA simulation predicts a solvent product composition of 0.0230 wt% compared to the co-current TSA simulation result of 0.00445 wt%. This is a direct result of the hot regenerant being at the feed composition for CZA and pure solvent for TSA. However, CZA has the advantage of not using any solvent.

The outlet composition graph for the salt HFA is shown in Fig. 5. In HFA mode, the same total hot time is used as in TSA and CZA. However, for the first part of the hot time, hot solvent is fed to the column while hot feed solution is added during the second part. Figure 5 is the result of using 3000 sec. of hot solvent followed by 3000 sec. of hot feed. The results of using different timings for the hot solvent and hot feed are discussed later. The maximum composition is 1.557 wt% and the average peak composition is 0.622 wt%, which is higher than co-current TSA and CZA. The solvent product composition is 0.00820 wt%, which is about twice that of co-current TSA, but only ∼36% of the CZA value.

Five additional results of interest are the solvent-to-feed usage ratio (S/F), the concentrated product-to-feed composition ratio ($c_{\text{Avg}}/c_{\text{F}}$), the solvent product-to-feed composition ratio ($c_{\text{pure}}/c_{\text{F}}$), the volumetric feed throughput to bed volume ratio (F/BV) and the energy use per cycle. These five value functions can be used to determine the feasibility of a particular system configuration. The results for all four configurations are given in Table 1. The CZA configuration has the advantage of not using any solvent. However, its composition ratios trail co-current TSA and HFA by significant margins and the solvent product is significantly less pure. HFA

Table 1. Results for liquid simulations for dilute aqueous sodium chloride feed.

Process	c_{Avg} (wt%)	c_{pure} (wt%)	Solvent/Feed	$c_{\text{Avg}}/c_{\text{F}}$	$c_{\text{pure}}/c_{\text{F}}$	F/BV	Energy (kW)
TSA (co-current)	0.611	0.00445	0.24	3.51	0.0256	39.50	343.6
CZA	0.591	0.023	0.0	2.98	0.1322	41.76	383.1
HFA	0.622	0.0082	0.111	3.57	0.0471	41.11	344.2
TSA (counter-current)	0.667	5.403E-4	0.251	3.83	0.0031	37.41	358.7

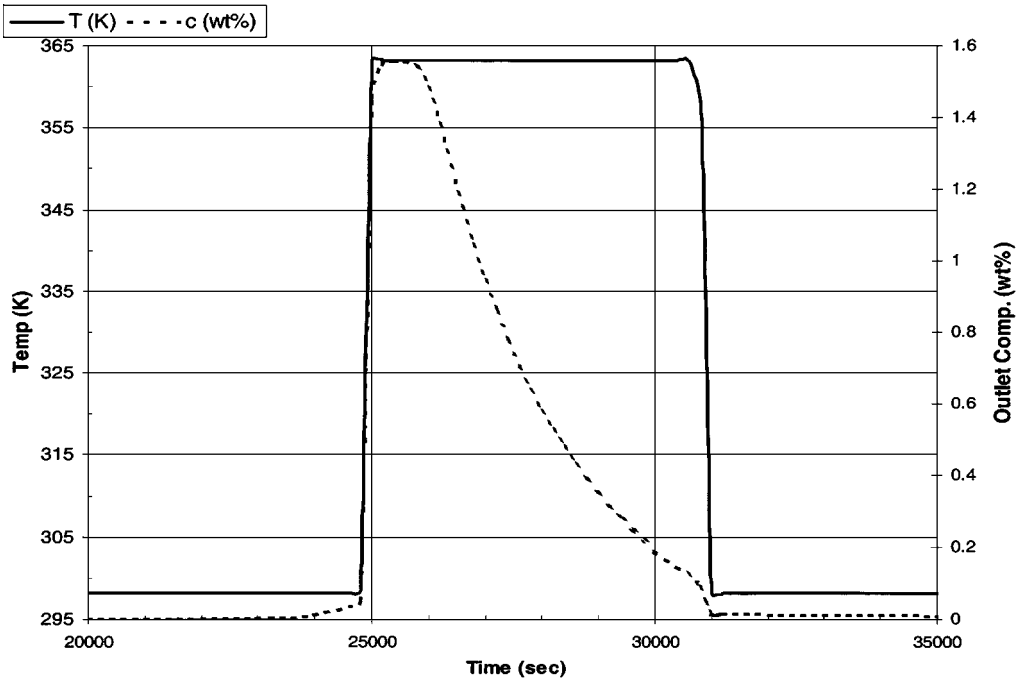

Figure 5. HFA composition and temperature profiles for dilute aqueous sodium chloride feed. Cold feed (25°C) for 22,210 sec., pure hot water (90°C) for 3000 sec., and hot feed (90°C) for 3000 sec.

surpasses co-current TSA in both $c_{\mathrm{Avg}}/c_{\mathrm{F}}$ and S/F value functions, but trails slightly in solvent product purity. The counter-current TSA configuration bested all other systems for the concentration ratios, but has the highest solvent usage. Counter-current TSA can process 10.4% less feed than CZA and 9.0% less feed than HFA. Although the energy use varies somewhat and is highest for CZA, in all cases it is about 3% of the energy required for doing an equivalent concentration by evaporation.

We are interested in seeing if there are situations where HFA out-performs counter-current TSA. To investigate this, the two configurations were compared based on equal amounts of hot solvent. For the liquid system, the first HFA step shown in Fig. 6 is to use 5000 sec. of solvent and 1000 sec. of feed for the hot step. The parallel to this for counter-current TSA is to use 5000 sec. of solvent for the hot step. At this point, counter-current TSA still has a slightly lower solvent product composition than HFA. However, as the hot feed time is increased for HFA (thus decreasing the solvent time), the results for counter-current TSA become markedly worse than HFA. Note in Fig. 6 that HFA with a hot solvent time of zero becomes CZA while HFA with a hot solvent time of 6000 sec. becomes co-current TSA.

Figure 6 can be used to determine which process is appropriate to use for a required solvent product composition. For composition requirements greater than 0.023 wt%, CZA would be the best choice. It provides a solvent product of more than sufficient purity and uses no pure solvent. Once the purity requirements become more stringent, HFA becomes the better choice. Purity requirements from 0.023 wt% down to 0.0045 wt% can be met with HFA using increasing portions of hot solvent. Up to this point, HFA out-performs counter-current TSA at corresponding hot solvent times. However, if extremely high purities are required (less than 0.004 wt% = 40 ppm), counter-current TSA is the better option with the restriction that solvent usage not be an issue, since large amounts of pure solvent are necessary to achieve these high purities. As a hypothetical example, suppose a product of 0.01 wt% is needed. According to Fig. 6, HFA requires about 2780 sec. of solvent to reach this purity level, while counter-current TSA needs about 4590 sec. of solvent. Counter-current TSA needs 65% more solvent to match HFA at this composition and HFA operation allows 3220 sec. of feed solution to replace pure solvent during its hot step. Since pure solvent would often be obtained from the product of the process, HFA produces more pure product.

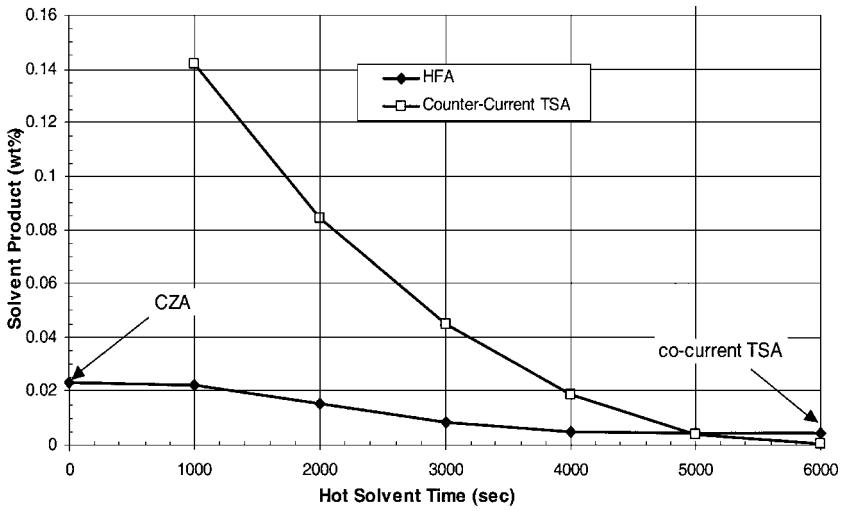

Figure 6. HFA vs. counter-current TSA results with same amount of hot pure water for dilute aqueous sodium chloride feed.

Simulation Results: Gas System

The gas system simulations all used a feed with a composition of $y_F = 0.003$ mole fraction benzene in nitrogen carrier gas at $T_F = T_c = 296.15$ K. Sorbonorit B activated carbon was used as the adsorbent (Yun et al., 2000). The purge gas used was pure nitrogen at a base temperature of $T_h = 467.44$ K, which is the characteristic temperature for this system. The hot addition periods for each configuration varied from 957 sec. to 1000 sec. per cycle. The outlet composition and temperature profiles for gas CZA are shown in Fig. 7. Note that, unlike Fig. 4, the composition wave exits before the thermal wave. This is typical of systems that focus. The maximum outlet mole fraction is 0.0191 and the average composition is 0.01128 mole fraction. The outlet profiles for co-current TSA and HFA are very similar to Fig. 7 (Natarajan, 2001) and are not shown.

The outlet composition profile and temperature at the top of the column for counter-current TSA are shown in Fig. 8. Due to the low velocity of the thermal wave, there is a pronounced shoulder at the feed concentration leading the concentration peak. Due to the design of a counter-current system, the shoulders in Figs. 3 and 8 cannot be removed by reworking the timing scheme. The maximum composition is 0.01985 mole fraction, the average mole fraction of the peak is 0.01044 and the carrier gas product composition is 6.727E-5 mole fraction. The final results for all four configurations are given in Table 2. As expected, CZA uses the least solvent and processes the most feed. However, counter-current TSA no longer produces the purest carrier gas product. HFA comes out on top for the purest carrier gas product. Unlike with the liquid system, CZA and HFA are very close for this gas system. The concentrated product composition of CZA is 2.68% higher than that of HFA, but the carrier gas product of HFA is 0.41% lower. For this separation with the specified regeneration temperature, CZA appears to be superior and can process 34.7% more feed than counter-current TSA. Further increases in the purge temperature cause smaller and smaller incremental increases in the amount desorbed during the purge step and do not appear to be advantageous.

Table 2. Results for gas simulations at $T_h = 467.44$ K for dilute feed of benzene in nitrogen.

Process	y_{Avg}	y_{pure}	Purge gas/Feed	y_{Avg}/y_F	y_{pure}/y_F	F/BV
TSA (co-current)	9.365E-3	8.037E-5	0.311	3.122	2.68E-2	690.3
CZA	0.01128	5.733E-5	0	3.759	1.911E-2	914.3
HFA	0.01097	5.709E-5	0.0757	3.658	1.903E-2	841
TSA (counter-current)	0.01044	6.727E-5	0.278	3.476	2.242E-2	678.7

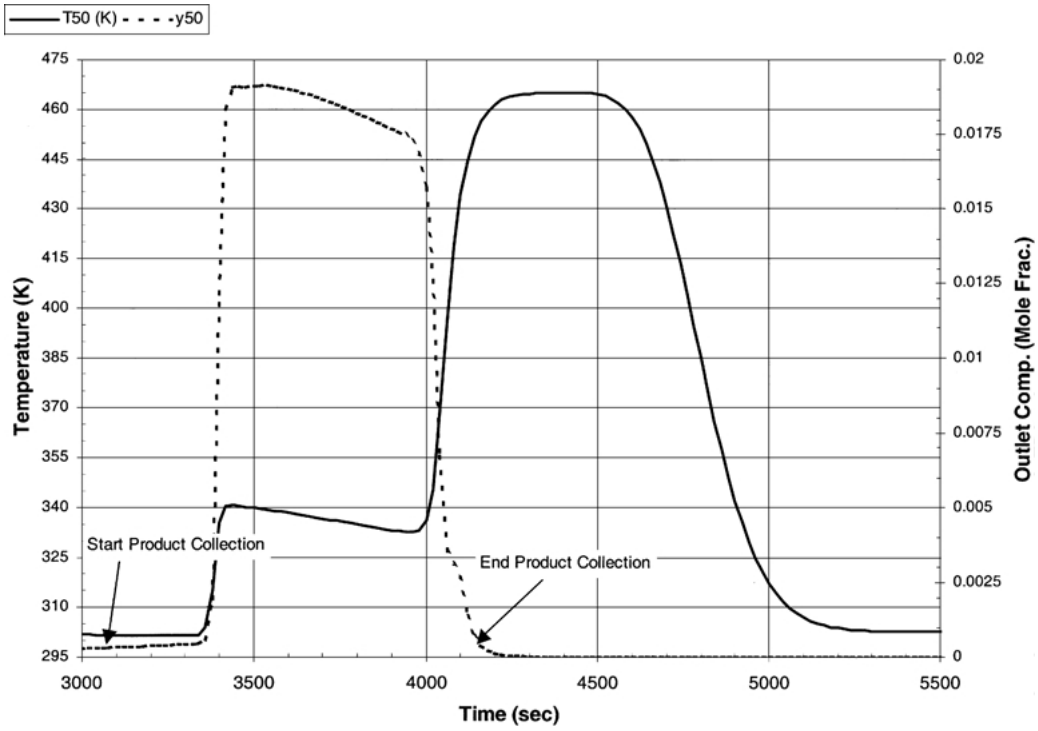

Figure 7. CZA composition and temperature profiles for dilute benzene in nitrogen feed. Cold feed (296.15 K) for 3156 sec. and hot feed (467.44 K) for 1000 sec.

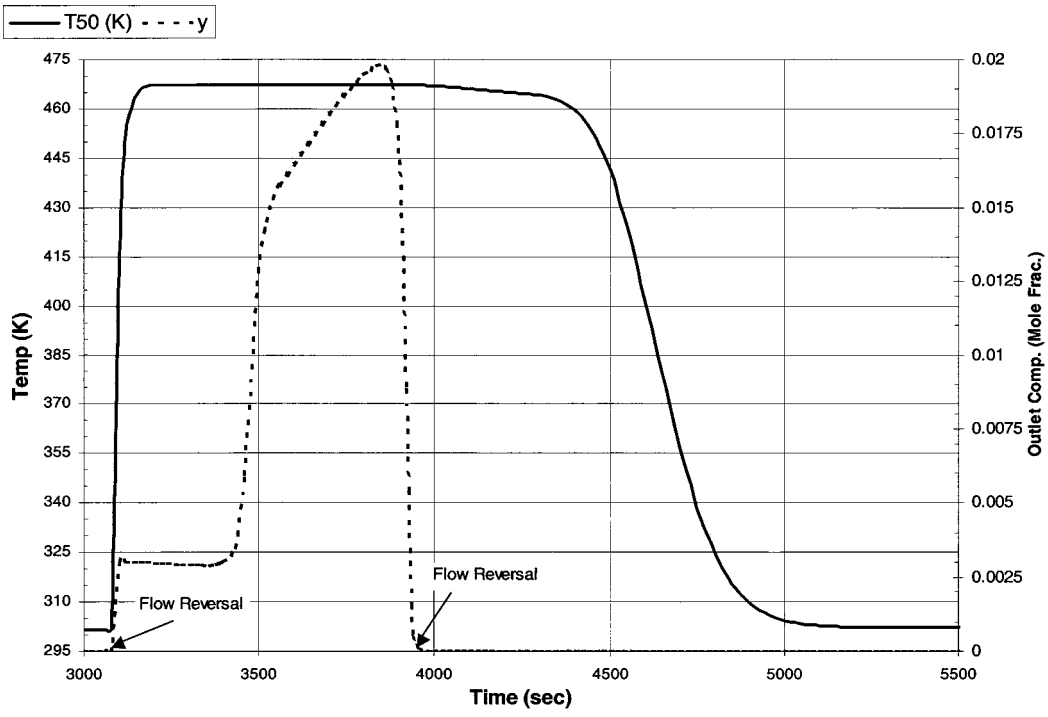

Figure 8. Counter-current TSA outlet composition and temperature at top of column for dilute benzene in nitrogen feed. Cold feed (296.15 K) for 3085 sec. and hot nitrogen (467.44 K) for 858 sec.

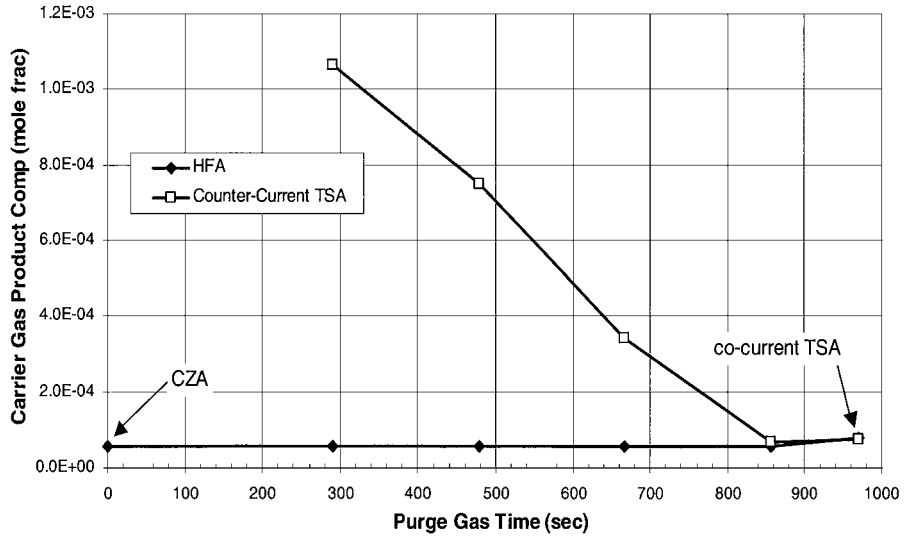

Figure 9. HFA vs. counter-current TSA for dilute benzene in nitrogen feed. $T_h = 467.44$ K.

Figure 9 shows a comparison of the processes with the same amount of hot pure purge gas. The trend is the same as for the liquid system: HFA is better than counter-current TSA until one approaches co-current TSA. The reason for the increase in the concentration of the carrier gas product for the counter-current process when purge time was increased from 857 sec. to 970 sec. is unclear, but could have been caused by the choice of cut points. Since repeated simulations gave the same result, this increase does not appear to be due to a mistake in the simulation. As the desorption step is shortened, less pure purge gas flows through the column, which limits the amount of the adsorbed solute that can be removed. HFA, on the other hand, makes up for the reduced pure purge gas time by using hot feed gas, maintaining the same total hot input time as co-current TSA. While there is an energy penalty incurred by heating the feed, there are savings in the amount of purge gas used by the process and more feed can be processed compared to counter-current TSA. The data presented in Table 2 show that the purge gas-to-feed ratio for HFA is lower than counter-current TSA. These results indicate that, in situations where purge gas recovery and usage are both important, HFA is clearly better than counter-current TSA. However, given favorable conditions such as focusing (which occurs in these gas simulations), the CZA limit is probably optimum, providing a high purity carrier gas product while not using any purge gas.

Discussion and Conclusions

Equations (1) to (3) can be simplified by making certain assumptions. The most important assumption is that the heat and mass transfer rates are very high. Thus, the solid and the stagnant fluid are locally in equilibrium. The result of this is that $q = \bar{q}$ and $c = c^*$ in Eqs. (1) and (2) and $T = T_s$ in Eq. (3). Additionally, the axial dispersion and diffusion terms are neglected, the velocity is assumed to remain constant and the heat of adsorption is neglected. With these assumptions the set of equations can be solved with the local equilibrium model (Natarajan, 2001; Wankat, 1990). The local equilibrium solutions agree qualitatively with the simulation results (Natarajan, 2001).

The performance of HFA varied significantly depending on the amount of feed solution used in the hot segment. At one extreme, CZA was the worst performer for the liquid system. It had the lowest concentrated product composition, the highest solvent product composition and the lowest solvent recovery factor. However, it does not use any pure solvent for the desorption step. At the other extreme, co-current TSA performed quite well, producing a more concentrated product and a purer solvent product than CZA. However, since it uses only pure solvent during the hot step, co-current TSA has the highest solvent-to-feed ratio. Between these two extremes, HFA proved to be a strong performer. It returned lower solvent-to-feed ratios and produced a more concentrated product than co-current

TSA. Counter-current TSA produced the most concentrated product and the purest solvent product at the expense of having the highest solvent usage. However, if a very pure solvent product is not required and the fresh solvent time is reduced, the solvent product composition for counter-current TSA increased rapidly, while HFA maintains a low solute content in the solvent product.

For the gas system, the results were slightly different. Due to the focusing phenomena observed at the temperatures used, CZA, the zero purge gas limit of HFA, produced the best results at the baseline simulation conditions. The concentrated product composition for CZA was better than HFA and the co-current TSA limit of HFA as well as counter-current TSA. The carrier gas product composition, however, was slightly higher than HFA. HFA produces a cleaner carrier gas product than counter-current TSA at all tested purge times. As with the liquid system, counter-current TSA requires long purge times to produce a clean carrier gas product.

Based on the results of the simulations, HFA will often be the best option to produce a concentrated liquid product of high purity while producing a relatively pure solvent product with minimal solvent usage. When extremely pure solvent product is required, counter-current TSA becomes the most attractive configuration for liquid systems. When focusing occurs in the gas system, CZA appears to be the best system. HFA has a great deal of flexibility since the amount of pure solvent or purge gas used can be adjusted between the limits of CZA and co-current TSA to meet a variety of system restrictions.

Nomenclature

a_p	Surface area to volume ratio (1/m)
$A(T)$	Isotherm parameter
$B(T)$	Isotherm parameter
c	Component concentration (kmol/m^3)
c_{Avg}	Average concentration
c_{F}	Feed concentration
c_{pure}	Solvent product composition
$C_{p,f}$	Fluid heat capacity (J/kg/K)
$C_{p,s}$	Solid heat capacity (J/kg/K)
E_z	Axial dispersion (m^2/s)
$E_{z,T}$	Thermal axial dispersion (m^2/s)
h_p	Lumped parameter heat transfer coefficient (m/s)
ΔH	Heat of adsorption (J/kg mole)
km	Lumped parameter mass transfer coefficient (m/s)
q	Amount of solute adsorbed (kmol/kg adsorbent)
T_c	Cold temperature (°C or K)
T_h	Hot temperature (°C or K)
y	Mole fraction
y_{Avg}	Average mole fraction
y_{F}	Feed mole fraction
y_{pure}	Purge gas product mole fraction

Greek Symbols

ε	Voidage
ρ_f	Fluid density (kg/m^3)
ρ_p	Particle density (kg/m^3)

Acknowledgments

Many thanks to Andrew Stawarz at Aspen Technology Inc. for his technical support, to Jeung-Kun Kim for reproducing simulations and to the National Science Foundation (Grant CTS-9815844) for providing part of the funding for this research.

References

Basmadjian, D., K.D. Ha, and C.-Y. Pan, "Nonisothermal Desorption by Gas Purge of Single Solutes in Fixed-Bed Adsorbers. I. Equilibrium Theory," *Ind. Eng. Chem. Process Des. Dev.*, **14**, 328–340 (1975).

Kayser, J.C. and K.S. Knaebel, "Recycled Thermal Swing Adsorption: Processes for Separation of Binary Mixtures," *Fundamentals of Adsorption*, A.I. Liapis (Ed.), pp. 307–318, Engineering Foundation, New York, 1987.

Knaebel, K.S. and R.L. Pigford, "Equilibrium and Dissipative Effects in Cycling Zone Adsorption," *Ind. Eng. Chem. Fundam.*, **22**, 336–346 (1983).

Matz, M.J. and K.S. Knaebel, "Recycled Thermal Swing Adsorption: Applied to Separation of Binary and Ternary Mixtures," *Ind. Engr. Chem. Res.,* **30**, 1046–1054 (1991).

Natarajan, G., "Thermal-Adsorptive Concentration," M.S. Ch.E. Thesis, Purdue University, West Lafayette, IN, 2001.

Schork, J.M. and J.R. Fair, "Parametric Analysis of Thermal Regeneration of Adsorption Beds," *Ind. Eng. Chem. Res.*, **27**, 457–469 (1988).

Tondeur, D., P. Jacob, D. Schweich, and P.C. Wankat, "The 'Guillotine Effect.' A New Concept in Chromatographic Separations," in *Proc. 2nd World Congr. Chem Eng.*, Vol. 4, pp. 226–230, Canadian Society for Chemical Engineering, 1981.

Wankat, P.C., *Rate Controlled Separations*, Chapters 6 and 8, Kluwer, Amsterdam, 1990.

Yun, J.-H., D.-K. Choi, and H. Moon, "Benzene Adsorption and Hot Purge Regeneration in Activated Carbon Beds," *Chem. Eng. Sci.*, **55**, 5857–5872 (2000).